



Universiteit
Leiden
The Netherlands

Pathogenesis and treatment of skeletal metastasis : studies in animal models

Buijs, J.T.

Citation

Buijs, J. T. (2009, January 21). *Pathogenesis and treatment of skeletal metastasis : studies in animal models*. Retrieved from <https://hdl.handle.net/1887/13413>

Version: Corrected Publisher's Version

License: [Licence agreement concerning inclusion of doctoral thesis in the Institutional Repository of the University of Leiden](#)

Downloaded from: <https://hdl.handle.net/1887/13413>

Note: To cite this publication please use the final published version (if applicable).

Chapter 6

Bone Morphogenetic Protein 7 in the Development and Treatment of Bone Metastases from Breast Cancer

Cancer Res 2007; 67:8742-51

Jeroen T Buijs¹,
Nico V Henriquez¹,
Petra GM van Overveld², Geertje van der Horst²,
Ivo Que¹, Ruth Schwaninger⁵,
Cyrill Rentsch⁵, Peter ten Dijke³,
Anne-Marie Cleton-Jansen⁴,
Keltouma Driouch⁶, Rosette Lidereau⁶,
Richard Bachelier⁷, Slobodan Vukicevic⁸,
Philippe Clézardin⁷, Socrates E Papapoulos¹,
Marco G Cecchini⁵, Clemens WGM Löwik¹,
Gabri van der Pluijm^{1,2}

Departments of Endocrinology¹, Urology²,
Molecular Cell Biology³ and Pathology⁴,
Leiden University

Medical Center, Leiden, The Netherlands;

⁵Department of Clinical Research and Urology,
University of Bern, Bern, Switzerland;

⁶Centre René Huguenin and Institut National
de la Santé et de la Recherche Médicale,
Research Unit 735, St.Cloud, France;

⁷Institut National de la Santé et de la
Recherche Médicale, Research Unit 664, Laennec;

School of Medicine, Lyon, France;

⁸Department of Anatomy,
School of Medicine, Zagreb, Croatia



Abstract

Bone Morphogenetic Protein 7 (BMP7) counteracts physiologic epithelial-to-mesenchymal transition (EMT), a process that is indicative of epithelial plasticity. Since EMT is involved in cancer we investigated whether BMP7 plays a role in prostate cancer growth and metastasis.

In this study we show that decreased BMP7 expression in primary breast cancer is significantly associated with the formation of clinically overt bone metastases in patients with ≥ 10 years follow-up. In line with these clinical observations, BMP7 expression is inversely related to tumorigenicity and invasive behavior of human breast cancer cell lines. Moreover, BMP7 decreased the expression of vimentin, a mesenchymal marker associated with invasiveness and poor prognosis, in human MDA-MB-231-B/Luc+ breast cancer cells under basal and TGF- β stimulated conditions. In addition, exogenous addition of BMP7 to TGF- β stimulated MDA-MB-231 cells inhibited Smad-mediated TGF- β signaling. Furthermore, in a well-established bone metastasis model using whole body bioluminescent reporter imaging, stable overexpression of BMP7 in MDA-MB-231 cells inhibited *de novo* formation and progression of osteolytic bone metastases and, hence, their metastatic capability. In line with these observations, daily intra-venous administration of BMP7 (100 $\mu\text{g}/\text{kg}/\text{day}$) significantly inhibited orthotopic and intra-bone growth of MDA-MB-231-B/Luc+ cells in nude mice.

Our data suggest that decreased BMP7 expression during carcinogenesis in the human breast contributes to the acquisition of a bone metastatic phenotype. Since exogenous BMP7 can still counteract the breast cancer growth at the primary site and in bone, BMP7 may represent a novel therapeutic molecule for repression of local and bone metastatic growth of breast cancer.

Introduction

Approximately 90% of cancer deaths result from the local invasion and distant metastasis of tumor cells¹. Better understanding of the process of metastasis is, therefore, urgently needed. Increased motility and invasiveness of breast cancer cells is reminiscent of the epithelial-to-mesenchymal transition (EMT) that occurs during embryonic development^{2,3}. This transition to a more mesenchymal, motile cellular phenotype is the result of a complex physiological process that includes dissolution of adherens junctions, loss of cell polarity, a change to spindle-like cell morphology, cytoskeletal reorganization, increased cell motility, loss of epithelial markers and induction of mesenchymal marker^{2,4}. Increased vimentin expression and perturbation of E-cadherin-mediated cell adhesion appear as hallmarks of this process⁴⁻⁸. However, in organogenesis 'mesenchymal' cells may possess remarkable plasticity and can eventually, regain a fully differentiated epithelial phenotype via a mesenchymal-to-epithelial transition (MET)⁹⁻¹¹.

Members of the transforming growth factor β (TGF- β) superfamily, which include bone morphogenetic proteins (BMPs), are involved in the control of many different biological processes including cell proliferation, differentiation, apoptosis and regulation of invasiveness¹²⁻¹⁴. In normal and non-malignant epithelial cells TGF- β is a potent growth inhibitor^{15,16}. However, different types of carcinomas often escape this tumor-suppressing activity and become refractile to growth inhibition^{15,16}. Even more, TGF- β can also potentiate tumorigenesis and contribute to the progression and invasiveness of various carcinomas^{8,17,18}. Accordingly, it has been shown that a blockade of TGF- β (signaling) inhibits tumor cell viability, migration, and metastasis¹⁹, including the formation of bone metastases^{20,21}. The homodimeric protein bone morphogenetic protein 7 (BMP7) induces MET in normal and non-transformed cells^{14,22}. For instance, during kidney development, BMP7 is essential for the condensation and epithelialization of the metanephric mesenchyme in the kidney, resulting in the formation of the tubular epithelium^{9-11,14}. Furthermore, BMP7 appears to be involved in the preservation of the epithelial phenotype^{23,24}, decreases fibrogenesis²³⁻²⁵, and causes repression of inflammation^{26,27}.

In this study, we present a crosstalk between BMP7 and TGF- β signaling in the regulation of EMT in breast cancer and identified BMP7 as a potential therapy for metastatic bone disease.

Materials and Methods

Cell line and Culture Conditions

The human breast cancer cell lines MDA-MB-231 (MDA-231), T47D and ZR-75-1 (ATCC, Rockville, USA) were cultured in DMEM (Gibco-BRL, Breda, The Netherlands) containing 4.5 g of glucose/L for MDA-231 or RPMI (ATCC, Rockville, USA) for T47D and ZR-75-1, supplemented

with 10% FCS (Gibco-BRL, Breda, The Netherlands), 100 units/ml penicillin and 50 µg/ml streptomycin (Life Technologies, Invitrogen, Breda, The Netherlands). Culture medium for T47D was supplemented with 6,5 µg/ml insulin (Sigma Chemical Co., St. Louis, MO, USA), and in culture medium for MDA-231-B/Luc+, a bone-seeking and luciferase expressing subclone from MDA-231²⁸, 800 µg/ml geneticin/G418 (Gibco-BRL, Breda, The Netherlands) was added. MCF10A²⁹ and its fully malignant derivative MCF10CA1a³⁰ (Barbara Ann Karmanos Cancer Institute, Detroit, MI, USA) were cultured as described previously³⁰. All cell lines were grown in a humidified incubator at 37°C and 5% CO₂. Mycoplasma contamination was regularly tested by PCR, but never detected.

Putative BMP7 effects on luciferase expression by MDA-231-B/Luc+ cells have been tested and excluded (data not shown).

Generation of isogenic BMP7-overexpressing cell lines using targeted integration

MDA-231 cells that display a unique predilection for bone (MDA-231-BO2³¹) were selected to generate a stable cell line that overexpresses BMP7. Stable cell lines were generated using the Flp-In system (Invitrogen, Breda, The Netherlands) according to manufacturer's protocol³². In short, a MDA-231-BO2-Flp-in host cell line (MDA-231-BO2-Frt11) was generated by stable introduction of a single copy of a Flp-Recombinase target (FRT) site as an integral part of an antibiotic resistance gene in the genome of these cells. Subsequently, a luciferase expressing subclone (MDA-231-BO2-Frt11/Luc+) was generated as described previously²⁸. This clone was used for the generation of isogenic stable cell lines by transient co-transfection of an FRT-targeting vector and a Flp-recombinase expression vector. The FRT-targeting vector was either a pcDNA5/FRT vector (Invitrogen, Breda, The Netherlands) expressing Green Fluorescent Protein (GFP) (control) or BMP7 (target gene) under the control of the CMV promoter. Due to Flp-mediated recombination at the genomic FRT-site, this targeting vector was incorporated in the genome. Simultaneously, a shift in antibiotic resistance was introduced allowing positive selection for integrants in the genomic FRT-site only and negative selection for random integrants in one single step³². This method allows the generation of isogenic stable cell lines, which only differ in sequence inserted in the genomic FRT site, thereby eliminating the need for clonal selection. It is important to note that both the MDA-231-BO2-Frt11 and MDA-231-BO2-Frt11/Luc+ cell line were validated for *in vivo* bone metastasis formation.

Patients

We retrospectively analyzed tumor tissue from 67 primary unilateral non-metastatic ductal breast carcinomas excised from women treated at Centre René Huguenin, St. Cloud, France from 1980 to 1994. The samples were examined histologically for the presence of tumor cells. A tumor sample was considered suitable if the proportion of tumor cells was more than 70%. Immediately after surgery, the tumor samples were stored in liquid nitrogen until RNA extraction.

Standard prognostic factors are presented in Table 1. All patients were treated by hormone therapy only after surgery. The patients had physical examinations and routine chest radiography every 3 months for the first 2 years, followed by annual examination (mammograms). The median follow-up was 11.2 years (range 1.5-20.3y). 35 Patients were without relapse (\geq 10 years of follow-up), 17 patients developed exclusively visceral metastases (liver and/or lung) and 15 patients developed exclusively bone metastases. Immunohistochemical validation was performed on fixed, paraffin-embedded tissue sections from primary breast tumor specimens (8/67).

Table 1 Characteristics of the 67 breast tumors from patients with and without relapse.

	Total population (%)	Number of patients with relapse (%)	P-values
Total	67 (100)	32 (47.8)	
Histological grade §			
I+II	48 (71.6)	22 (45.8)	n.s.
III	17 (28.4)	10 (58.8)	
Lymph node status			
Node-negative	13 (19.4)	1 (7.7)	P=0.0072
Node-positive 1-3	34 (50.7)	18 (52.9)	
Node-positive >3	20 (29.9)	13 (65)	
Clinical tumor size			
\leq 30mm	25 (37.3)	7 (28)	P=0.040
>30mm	42 (62.7)	25 (59.5)	
Estrogen receptor status			
Negative	9 (13.4)	4 (44.4)	n.s.
Positive	58 (86.6)	28 (48.3)	
Relapses			
+	32 (15 with bone mets)		
-	35		

§ Scarff Bloom Richardson classification, n.s. = not significant.

Enzyme-linked immunosorbent assay (ELISA) for human BMP7

Levels of BMP7 in conditioned media were measured with a commercially available specific ELISA kit using sandwich enzyme immunoassay technique (R&D systems, Abingdon, United Kingdom). Cells were routinely cultured for 4 days.

Real-Time RT-PCR

Total RNA was extracted with the RNeasy Midi kit (Qiagen, Venlo, The Netherlands) from *in vitro* cultured cells at 70-80% confluence. Reverse transcription was performed with random primers in the presence of RNase inhibitor (Roche Diagnostics, Rotkreuz, Switzerland). Quantitative real-time RT-PCR (qPCR) was performed using commercially obtained exon-specific primers for BMP7, E-cadherin, vimentin, and β -actin (primer catalog numbers:

Hs 002333477 m1, Hs 00170423 m1, Hs 00185584 m1 and Hs 99999903 m1, respectively; Applied Biosystems, Rotkreuz, Switzerland) on an ABI Prism 7700 sequence detection system (Applied Biosystems, Rotkreuz, Switzerland). All experiments were performed in duplo on 4 different samples. For BMP7 mRNA detection in patients, qPCR (incl. thermal cycling conditions) was performed as described previously³³. Each sample was normalized on the basis of its TATA box-binding protein (TBP) content. Primers used: BMP7 fwd ATG GCC AAC GTG GCA GAG AA, BMP7 rev CAG CCC AGG TCT CGG AAG CT, TBP fwd TGC ACA GGA GCC AAG AGT GAA and TBP rev CAC ATC ACA GCT CCC CAC CA. All qPCR values were normalized using the comparative method of Livak and Schmittger³⁴.

Western Blot

Cells were seeded in 6-wells plates at a density of 20.000/cm² in DMEM with 0.1% Fetal Clone II (FCII; HyClone, Perbio Science Nederland B.V., Etten-Leur, The Netherlands) for MDA-231-B/Luc+. After 18 hours, cells were stimulated with recombinant human mature BMP7 (rhBMP7)³⁵ (0.5 mg batches, Creative Biomolecules, Hopkinton, MA, USA; rhBMP7 was freshly dissolved to a stock solution – 1 mg/ml in 20 mM acetate buffer with 5 % mannitol, pH 4.5 – and was obtained from Dr. Vukicevic) and/or porcine TGF- β 2 (R&D systems, Uithoorn, The Netherlands). After an additional 48 hours, cells were lysed and collected in 250 μ l lysisbuffer (20 nM Tris pH 7.5; 20% glycerol; 400 mM KCl; 1 nM DTT; aprotinin (1/1000) and Roche protease inhibitor mix) followed by one or two rounds of freeze/thawing, and used for Western Blot analysis as described earlier³⁶. Rabbit polyclonal antibodies α -vimentin (diluted 1:500; ab7783, Abcam, Cambridge, UK) and α -E-cadherin (diluted 1:500; sc-7870, Santa Cruz Biotechnologies, Tebu-bio, Heerhugowaard, The Netherlands), and a mouse monoclonal antibody α -beta-actin (clone AC-15, Sigma-Aldrich, Zwijndrecht, The Netherlands) were used as primary antibodies.

Cells Grown on Chamber Slides

MDA-231-B/Luc+cells were seeded at a density 20.000/cm² in DMEM with 0.1% FCII in 8 chamber slides (Falcon, Becton Dickinson, Etten-Leur, The Netherlands), and growth factors were added after 18 hours. After 30 hours, cells were dried for 5 minutes and fixed with 3.7% paraformaldehyde (pH 6.8) (Merck, VWR, Amsterdam, The Netherlands) in PBS for 10 minutes and stained for vimentin as described for tissues, with the exception of the antigen retrieval step (see section 'histomorphometry, histochemistry and immunohistochemistry'). Images were acquired using a color charged-coupled device (CCD) camera mounted on a Nikon Eclips 610 microscope at a twenty-fold magnification. Subsequently, cells were scored double-blind for positive vimentin staining from four randomly chosen fields by two investigators (J.B. and P.v.O.).

Transient transfections and transcription reporter assays

MDA-231 cells were seeded at a density 7.500 cells /cm² in DMEM with 10% FCII in 24-well plates. On the subsequent day, cells were transiently transfected with 1µg of the indicated constructs using FuGENE 6 (Roche, Mannheim, Germany) transfection reagent following manufacturer's protocol. To correct for transfection efficacy, 100 ng of renilla luciferase (pRL-CMV; Promega, Madison, WI, USA or pRL-CAGGS, Promega, Madison, WI, USA) was co-transfected. On day 3, cells were serum starved for 24 hours before stimulation with TGF-β and/or BMP7 for a duration of 30 hours. On day 5, luciferase activities were quantified using Dual Luciferase Assay (Promega, Madison, WI, USA)³⁷. Firefly luciferase activity was corrected for renilla luciferase activity. The experiments were performed in four fold and repeated at least twice. Values are expressed as means ± s.e.m.

Luciferase Reporter Gene Constructs

For intracellular signaling of TGF-β the *CAGA-luciferase* construct, consisting of 12 Smad3/Smad4 binding sequences (CAGA boxes) and the luciferase-coding sequence was used. The CAGA boxes confer TGF-β stimulation to a heterologous promoter reporter construct, whose activity depends on binding of activated Smad3/Smad4 transcription factor complexes³⁷. The *BRE-luciferase* construct, that is based on the mouse Id1 promoter, was used to study the presence and functionality of BMP-receptors³⁸.

Proliferation Assay

Cells were seeded in 96-wells plates at a density of 4.000/cm². 18 Hours after MDA-231-B/Luc+cells were seeded, cells were stimulated with 500 ng/ml BMP7 for 72 hours. Proliferation was measured with the CellTiter 96 Aqueous Non-Radioactive Cell Proliferation Assay (Promega, Madison, WI, USA) according to manufacturer's protocol.

Animals

Female nude mice (BALB/c *nu/nu*) were purchased from Charles River (L'Arbresle, France). Animals were housed in individual ventilated cages under sterile condition, and sterile food and water were provided *ad libitum*. Animal experiments were approved by the local committee for animal health, ethics and research of Leiden University and carried out in accordance with European Communities Council Directive 86/609/EEC. For surgical and analytical procedures mice were anaesthetized by intra-peritoneal injection of a 50 µl 1:1:1 mixture; Ketamine HCl (Stock solution of 100 mg/ml Nimatek; Vetimex Animal Health B.V., Bladel, The Netherlands.) + Xylazine (2% Rompun, Bayer AG, Leverkusen, Germany) + PBS (pH 6.8). At the end of the experimental period animals were sacrificed by cervical dislocation.

Animal Models

All cells were harvested at 70-80% confluence after changing to geneticin-free medium 24 hours before inoculation.

For tumor growth in the bone marrow, single cell suspensions 2.5×10^5 MDA-231-B/Luc+cells/ 10 μ l PBS were injected into the right tibiae of 6-week old mice as described previously^{28,39}.

Three days after intraosseous (i.o.) inoculation of MDA-231-B/Luc+cells the animals were equally distributed into three experimental groups based on a comparable tumor burden/mouse, as detected by whole body bioluminescent reporter imaging (BLI). From this time point (day 0), and during a subsequent period of 24 days, all animals received vehicle or rhBMP7 (10 μ g/kg/day or 100 μ g/kg/day) treatment by tail vein injection. The progression of intraosseous growth was monitored by BLI at day 3, 10, 17 and 24 and by radiography at day 17 and 2^{28,39}.

6-Weeks old mice were also i.o. inoculated (1.0×10^5 cells/ 10 μ l PBS) with either MDA-231-B02-Frt11(GFP)/Luc+ cells (n=8) or MDA-231-B02-Frt11(BMP7)/Luc+ cells (n = 5). The progression was monitored by BLI weekly and by radiography at the end of the experiment (day 28)^{28,39}.

For orthotopic tumor growth, single-cell suspensions of 1.0×10^6 MDA-231-B/Luc+cells/ 10 μ l PBS were inoculated via a 0.5 ml U-100 insulin needle (29G $\frac{1}{2}$, BD Micro-Fine, Becton Dickinson, Etten-Leur, The Netherlands) into the mammary fat pads of 7-week old mice. Animals were equally distributed into two experimental groups based on a comparable tumor burden/mouse, as detected by BLI. From this time point (day 0), all animals were given vehicle or BMP7 (100 μ g/kg/day) treatment by tail vein injection. Subsequently, the progression of orthotopically growing tumors was monitored weekly by BLI^{28,39}.

4.5-Weeks old nude mice were inoculated (5.0×10^5 cells/ 100 μ l PBS) in the tail artery with either MDA-231-B02-Frt11(GFP)/Luc+ cells (n=13) or MDA-231-B02-Frt11(BMP7)/Luc+ cells (n=8), as described earlier³¹. The progression was monitored by BLI weekly and by radiography at the end of the experiment (day 28)^{28,39}.

After the experimental periods, mice were sacrificed by cervical dislocation.

Mammary fat pads and tibiae with tumors were dissected and processed for further histomorphometrical and immunohistochemical analysis (see below).

Whole Body Bioluminescent Reporter Imaging of Isogenic BMP7- and GFP-Overexpressing Cell lines

In animals that were inoculated with either MDA-231-B02-Frt11(GFP)/Luc+ or MDA-231-B02-Frt11(BMP7)/Luc+, the luciferase activity was visualized through imaging of whole bodies with an intensified-charge-coupled device (I-CCD) video camera of the *in vivo* Imaging System (IVIS 100, Xenogen, Alameda, CA, USA). The animals were anesthetized using the isofluorane anesthesia system (XGI-8, Xenogen), and injected intra-peritoneally with 2 mg D-luciferin sodium salt (Synchem OHG, Felsberg/Altenburg, Germany) dissolved in

PBS. Animals were kept anesthetized, and measurements were performed 5 min after the injection of D-luciferin. Bioluminescence imaging was acquired with a 15-cm FOV, a medium binning factor, and exposure times of 10–60 s. Imaging data were analyzed by using the program living image (Xenogen, Alameda, CA, USA). Values are expressed as relative light units (RLU) in photons/sec.

Radiographical Analysis

Radiographic analyses of osteolytic lesions were assessed by radiography (Kodak X-OMAT TL film, Eastman Kodak Company, Rochester NY) using a Hewlett Packard X-ray system Faxitron 43805, and quantified using NIH-Image 1.62b7 software as described earlier³⁹.

Histomorphometry, Histochemistry and Immunohistochemistry

After orthotopic tumors and bone metastasis were fixed in 3.7% paraformaldehyde (pH 6.8) in PBS and processed, they were submitted to Goldner staining, staining for tartrate-resistant acid phosphatase (TRAcP), H&E staining or immunohistochemical staining as described previously^{39,40}. Histomorphometric measurements of tumor burden were performed on central sections through the tumor (largest tumor area). Tumor growth in bone could be readily identified by pancytokeratin staining alone or in combination with H&E staining. Total tumor areas, as an estimate of total tumor burden, was measured by image analysis using NIH-Image 1.62b7 image analyses software as described previously³⁹. Subsequently, a distinction was made between the total tumor burden and the intraosseous and extraosseous tumor burden as described previously³⁹.

The following rabbit polyclonal antibodies were used at a concentration of 10 µg/ml: α-human pan-cytokeratin (DAKO, Heverlee, Belgium), α-human vimentin (ab7783, Abcam, Cambridge, UK), α-human BMP7 (2854ab, directed against pro-domain of BMP7, obtained from Dr.Vukicevic)^{35,41}, α-phosphorylated Smad1 (PS1)⁴² and normal rabbit IgG (Jackson Immuno Research, Cambridgeshire, UK) antibodies as negative control. Goat α-rabbit IgG (DAKO, Heverlee, Belgium) was used as secondary antibody. For antigen retrieval, slides were treated for 10 minutes at 37°C with 5 µg/ml proteinase K (Gibco-BRL, Breda, The Netherlands). To quantify PS1 and TRAcP staining, three histological sections per mouse (n=8) were acquired using a color CCD camera mounted on a Nikon Eclipse 610 microscope at a twenty-fold magnification. Subsequently, the number of cells that stained positive was scored single-blind by two investigators (G.v.d.P. and P.v.O.).

BMP7 staining on patient material was performed similarly, except that 5% normal goat serum (Jackson Immuno Research, Cambridgeshire, UK)/ 0.5% Boehringer Milk Powder (Boehringer Mannheim, Mannheim, Germany)/ TTBS was used instead of 0.5% Boehringer Milk Powder/ TTBS for incubation and first antibody dilution, and 0.01 M citrate buffer (pH 6.0) (7 minutes at 98°C) was used as antigen retrieval step, unless stated otherwise.

Statistical Analysis

Survival rates were determined using the log-rank test. Since BMP7 mRNA levels in patients did not follow a Gaussian distribution, (a) the mRNA levels in each subgroup of samples were characterized by their median values and ranges, rather than their mean values and coefficients of variation, and (b) relationships between the molecular markers and clinical and histological parameters were tested using the non-parametric Mann-Whitney *U* test. Other data are represented as mean \pm s.e.m.. *In vivo* tumor growth was measured by general linear model with repeated measurements using a LSD *post-hoc* test when applicable. Other statistical evaluations were carried out by ANOVA using a LSD *post-hoc* test when applicable.

Results

BMP7 Expression in Human Primary Breast Cancer and Formation of Distant Metastasis

BMP7 mRNA expression levels in primary breast tumors developing bone or visceral metastases were not significantly different from breast cancer patient without relapse (column 2 vs. 1, Table 2), and there was no significant difference observed that patients with primary breast tumors developing bone metastases had lower BMP7 mRNA expression levels ($p = 0.13$; column 3 vs. 1, Table 2) than patients without relapse. However, BMP7 mRNA expression levels in primary breast tumors developing bone metastases were significantly lower when compared to primary breast tumors developing visceral (lung and/or liver) metastases ($p = 0.027$; column 3 vs. 4, Table 2).

Table 2 BMP7 mRNA expression levels in human primary breast carcinomas as detected by qPCR. Median (range) of mRNA levels

1	2	3	4
Breast tumor without metastasis (n=35)	Breast tumor with metastasis (n=32)	Breast tumor with bone metastasis (n=15)	Breast tumor with visceral metastasis (n=17)
1.0 (0.03 - 85.92)	0.83 (0.01 - 11.43) #	0.48 (0.01 - 3.71)	1.40 (0.17 - 11.43) *

#, n.s. (column 1 vs. 2); *, $p = 0.027$ (column 3 vs. 4)

In patient matched normal ducts of the breast, apical BMP7 staining could be observed (Fig. 1, *upper panels*). Staining intensity of BMP7 protein in primary breast cancer specimens was in accordance with BMP7 mRNA levels (Fig. 1, *middle panels*). Adult kidney were used as positive (Fig. 1, *left bottom panel*) and negative (Fig. 1, *right bottom panel*) control.

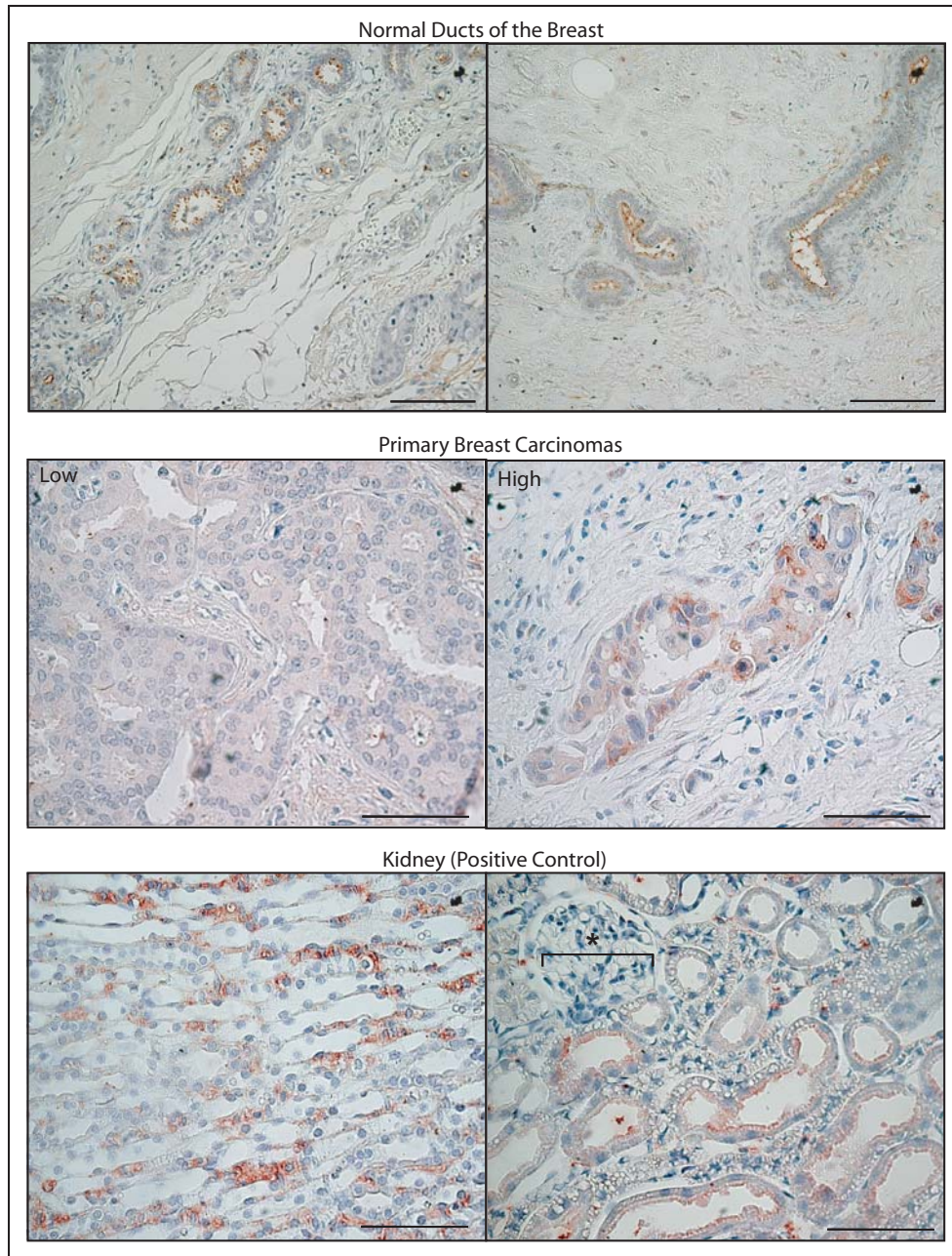


Figure 1 **BMP7 mRNA expression levels and BMP7 immunolocalization in human primary breast cancer.** BMP7 immunolocalization. Upper panels, normal ducts of the breast (Pronase [0.1% for 10 minutes at 37°C, Roche] was used as antigen retrieval step). Immunolocalization of BMP7 in primary breast tumors with low (left middle panel) and high (right middle panel) levels of BMP7 mRNA (0.09 and 16.11, respectively). Rat kidney: medullary rays were used as a positive (left bottom panel) and glomeruli (as indicated by *) as negative control (right bottom panel). Adjacent to the negative glomerulus, convoluted tubuli stained positive for BMP7. Scale bars in upper left panel 80 μm , scale bars in other panels 50 μm .

Tumorigenicity and BMP7 Expression *In Vitro*

We investigated whether BMP7 expression in human breast cancer cell lines is associated with tumorigenic and metastatic potential. The six cell lines examined in this study have progressively greater tumorigenic and metastatic potential when arranged in the following order: MCF10A (normal breast epithelial cells), ZR-75-1, T47D, MCF10CA1a, MDA-231 and MDA-231-B/Luc+, where MCF10CA1a, MDA-231 and its derivative MDA-231-B/Luc+ are highly tumorigenic and metastatic. This arrangement of the cell lines inversely correlates with the expression of BMP7 (Fig. 2A). E-cadherin/vimentin expression ratios, indicative of epithelial phenotype, are also inversely related to BMP7 expression (Fig. 2A), suggesting that acquisition of an invasive phenotype coincides with decreased BMP7 expression.

Immunohistochemical staining of MDA-231-B/Luc+ cells for vimentin demonstrated a heterogeneous population with 22% vimentin positive (Vim+) cells (Fig. 2B). Stimulation with BMP7 significantly decreased the percentage of Vim+ cells (5%; $p = 0.038$ versus control), while stimulation with TGF- β significantly increased the percentage of Vim+ cells (49%; $p = 0.002$ versus control). This increase in vimentin expression by TGF- β could be blocked completely by co-incubation of BMP7 (12% Vim+ cells; $p < 0.001$ versus TGF- β treated cells). These results were further confirmed by Western Blotting (Fig. 2C).

Next we tested whether BMP7 acts on MDA-231 cells to inhibit the acquisition of an invasive, mesenchymal phenotype by antagonizing Smad-dependent TGF- β signaling.

The presence of functionally active TGF- β receptor complexes, particularly ALK5, in MDA-231 cells was demonstrated by the dose-dependent activation of the CAGA-luciferase reporter, whose activity depends on activated Smad3/4 transcription factor complexes (Fig. 2D). Addition of BMP7 to TGF- β -stimulated MDA-231 cells significantly inhibited the TGF- β -driven CAGA-luciferase activity ($p < 0.001$).

Addition of BMP7, but not TGF- β , stimulated BRE4-luciferase activity, indicating the presence of functioning, activated type I BMP-receptor complexes in MDA-231 cells (Fig. 2D). TGF- β antagonizes BMP7 induced BRE-luciferase activity ($p < 0.001$).

It is important to note that BMP7 did not affect proliferation of MDA-231-B/Luc+ cells *in vitro* using different cell culture conditions (1% FCS and 10% FCS; Suppl. Fig. 1).

BMP7 overexpression and Experimental Bone Metastasis

As detected with ELISA, overexpression of BMP7 in MDA-231 cells (MDA-231-B02-Frt11(BMP7)/Luc+) resulted in substantial secretion of BMP7 protein in the medium, 6.55 ng BMP7 protein/ 1E6 cells/ day. In contrast, BMP7 protein was not detectable in the control cell line (MDA-231-B02-Frt11(GFP)/Luc+), < 0.03 ng BMP7 protein/ 1E6 cells/ day.

Overexpression of BMP7 in MDA-231 cells (MDA-231-B02-Frt11(BMP7)/Luc+) significantly inhibited both the intra-bone growth ($p = 0.034$), osteolytic area ($p = 0.007$), and extraosseous extension ($p = 0.042$) when compared to control (MDA-231-B02-Frt11(GFP)/Luc+) (Fig. 3A). Moreover, in an experimental model of bone metastasis using tail inoculation of breast can-

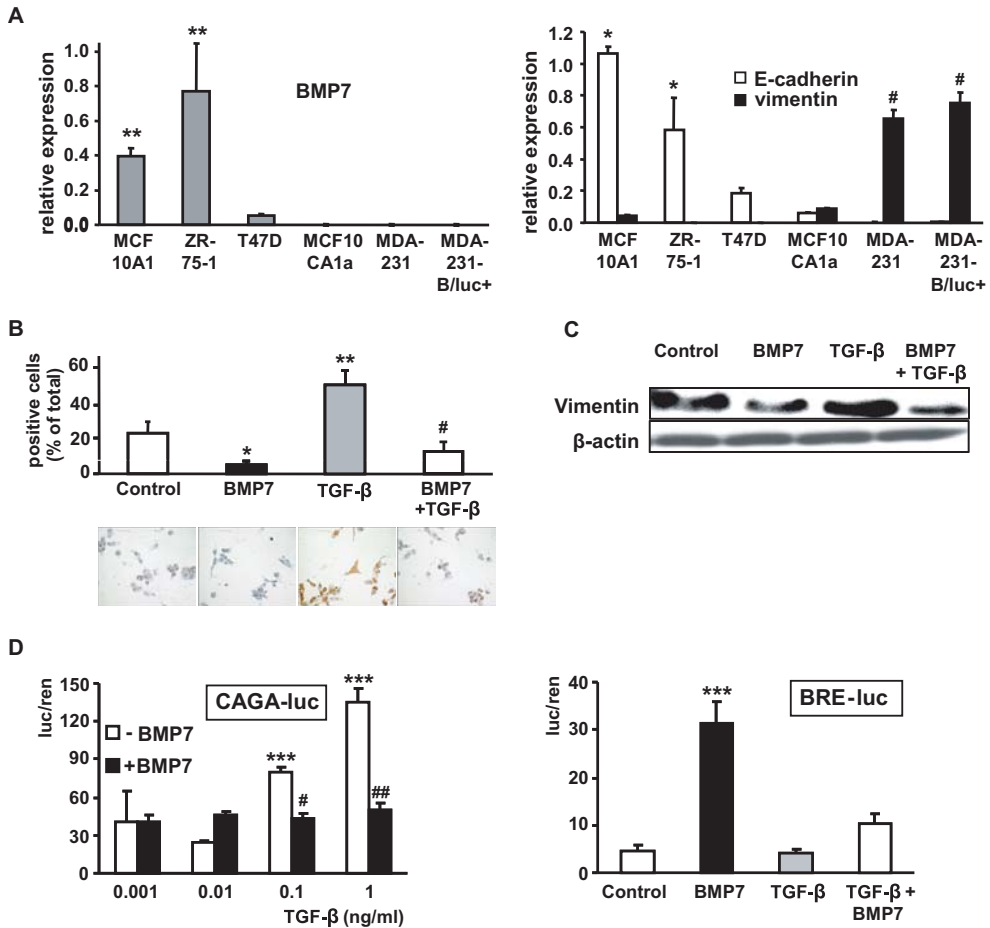


Figure 2 **E-cadherin and vimentin expression in breast cancer cell lines.** *A*, BMP7, E-cadherin and vimentin mRNA expression in human breast cancer cell lines with increasing tumorigenic and metastatic potential (left to right) as detected by qPCR. E-cadherin expression in MDA-231 and MDA-231-B/Luc+ cells, vimentin expression in T47D and ZR-75-1 cells, and BMP7 expression in MCF10CA1a, MDA-231 and MDA-231-B/Luc+ cells were just above detection level. ** $p < 0.01$ versus BMP7 expression in T47D, MCF10CA1a, MDA-231 and MDA-231-B/Luc+ cell lines. * $p < 0.05$ versus E-cadherin expression in all other cell lines; # $p < 0.01$ MDA-231 cell lines versus the other cell lines; Expression values are normalized to β -actin (BMP7/ 10^3 β -actin). *B*, vimentin immunolocalization of MDA-231-B/Luc+ cells after incubation with 1 μ g/ml BMP7 in the presence or absence of 10 ng/ml TGF- β . Representative examples are shown. *C*, expression of vimentin by MDA-231-B/Luc+ cells after incubation with 1 μ g/ml BMP7 in the presence or absence of 10 ng/ml TGF- β as detected by Western Blotting. * $p < 0.05$ and ** $p < 0.01$ versus control, # $p < 0.001$ versus TGF- β , n.s. = not significant. *D*, MDA-231 cells were transiently transfected with the CAGA-luciferase reporter (left panel) and the BRE-luciferase reporter (right panel) constructs. The presence of functionally active TGF- β receptor complexes was demonstrated with stimulation of the CAGA-luc reporter by TGF- β (***) $p < 0.001$ vs. all other conditions). Addition of BMP7 (500 ng/ml) to TGF- β -stimulated MDA-231 cells significantly (# $p < 0.01$, ## $p < 0.001$) inhibited TGF- β -driven CAGA-luc activity. Values are normalized to renilla [CAGA-luc/ 10^5 pRL-CAGGS]. Value vehicle treated is 16.1 ± 1.1 . BMP7 (200 ng/ml), but not TGF- β (5 ng/ml), induces BRE-luc activity, indicating the presence and functionality of BMP-receptors in MDA-231 cells. (***) $p < 0.001$ vs. all other conditions; values are normalized to renilla [BRE4-luc/ 10^1 pRL-CMV].

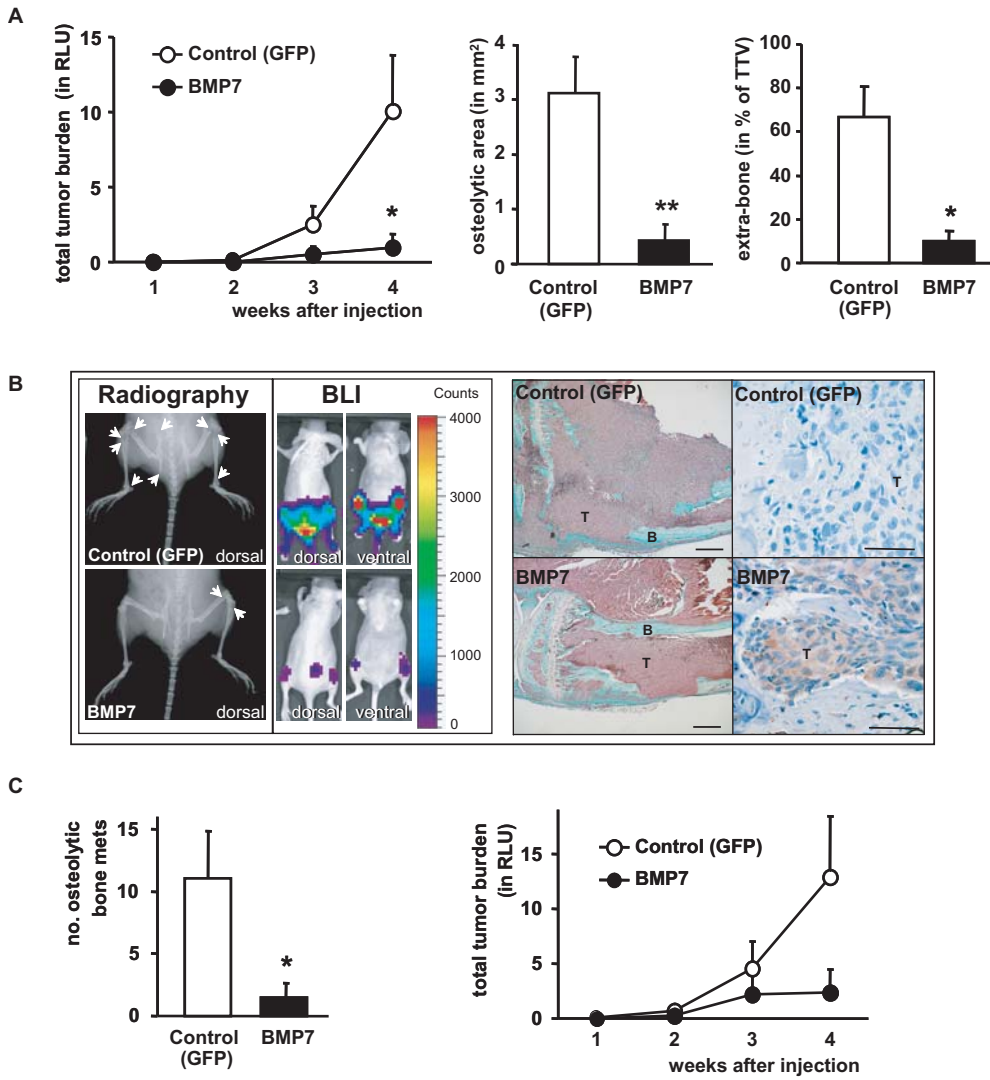


Figure 3 Bone metastatic and intra-bone growth of MDA-231 cells expressing BMP7. *A*, in an experimental model of intraosseous implantation of breast cancer cells, stable BMP7 overexpression inhibited osteolysis as detected by radiographical analysis, total tumor burden as measured by BLI (RLU: 10^6 photons/sec), and extraosseous tumor volume determined as the percentage of total tumor volume (TTV) that has started to grow extramedullary. *B*, experimental model of bone metastasis formation after tail inoculation of breast cancer cells, from which representative examples of radiography, BLI, Goldner staining (scale bars 200 μ m) and BMP7 immunolocalization (scale bars 50 μ m) (from left to right) are shown. Arrows indicate osteolytic lesions; T = tumor; B = bone. *C*, in the experimental bone metastasis model stable BMP7 overexpression inhibited de novo formation of osteolytic bone metastases (per mouse) as detected by radiographical analysis, and total tumor burden (per mouse) as measured by BLI (RLU: 10^6 photons/sec). * $p < 0.05$ and ** $p < 0.01$ versus control (GFP).

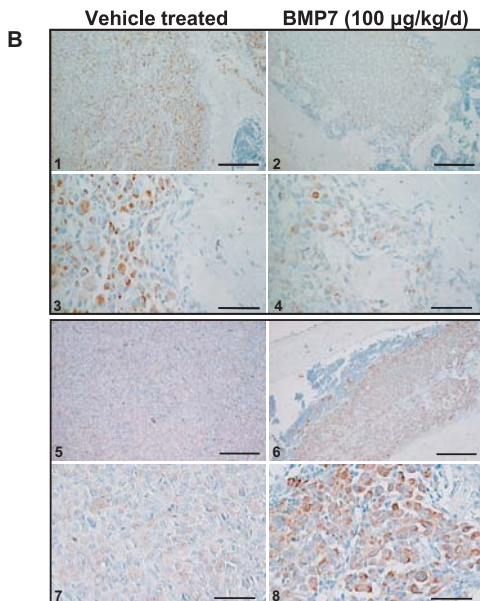
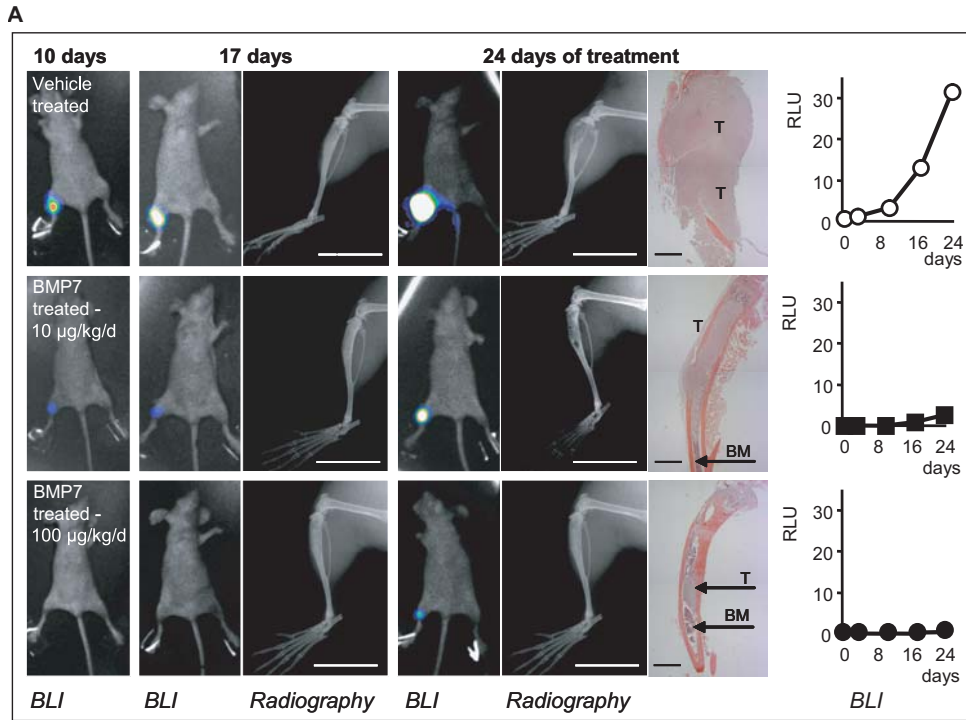


Figure 4 Representative examples of BMP7 treatment and intra-bone growth of MDA-231-B/Luc+cells. *A*, intra-bone growth of tumor cells and tumor-induced osteolysis (BLI, radiography and histology). In the graphs, BLI is quantified in relative light units (RLU) (10^5 photons/sec). Scale bars in X-rays: 10 mm; scale bars in histological sections: 1 mm. T = tumor, BM = bone marrow. *B*, expression of vimentin [1-4] and pan-cytokeratin [5-8] in MDA-231-B/Luc+cells growing in bone marrow after vehicle [1,2,5,6] and 100 µg/kg/d BMP7 [3,4,7,8] treatment. Scale bars in 1,2,5,6: 150 µm, scale bars in 3,4,7,8: 40 µm.

cer cells, overexpression of BMP7 in MDA-231 cells (MDA-231-B02-Frt11(BMP7)/Luc+) was shown to significantly inhibit the number of osteolytic lesions ($p = 0.025$; Fig. 3B,C). In line with the ELISA data described above, overexpression of BMP7 protein in tumor cells was also detected in histological sections in bone metastasis from MDA-231 cells overexpressing BMP7 (MDA-231-B02-Frt11(BMP7)/Luc+), but not in the GFP-control cell line (Fig. 3B). In addition, a trend was noticed for less overall total tumor burden as detected by BLI ($p = 0.10$; Fig. 3C). Furthermore, it is important to note that BMP7 overexpression did not affect the growth rate *in vitro* (doubling time MDA-231-B02-Frt11(BMP7)/Luc+ cells: 21.0hr, vs. MDA-231-B02-Frt11(GFP)/Luc+ cells: 20.9hr).

Experimental BMP7 Treatment

Fig. 4 depicts a representative example from each experimental group (vehicle treatment, 10 $\mu\text{g}/\text{kg}/\text{day}$ BMP7 or 100 $\mu\text{g}/\text{kg}/\text{day}$ BMP7) showing different *in vivo* imaging methods (BLI, radiography, histology) that have been used to detect MDA-231-B/Luc+ breast cancer cells growing in bone. Breast cancer growth in bone and the formation of osteolytic lesions was strongly inhibited, particularly in the high dose BMP7 group (100 $\mu\text{g}/\text{kg}/\text{day}$ BMP7) (Fig. 4A). Markedly, mice receiving 100 $\mu\text{g}/\text{kg}/\text{day}$ BMP7 had tumors that express higher levels of cytokeratins and lower levels of vimentin when compared to vehicle treated mice (Fig. 4B). The number of strong cytokeratin-positive cells was increased by 25% upon BMP7 treatment. This indicates that BMP7 treatment provokes a more epithelial-like phenotype.

In the vehicle treated group, the tumor burden increased strongly over time (Fig. 5A). Tumor growth in mice receiving 10 $\mu\text{g}/\text{kg}/\text{day}$ BMP7 was not significantly different from vehicle treated animals, whereas 100 $\mu\text{g}/\text{kg}/\text{day}$ BMP7 strongly and significantly inhibited tumor progression ($p = 0.038$; Fig. 5A). This result was confirmed by histomorphometric analysis of total tumor burden ($p = 0.049$; Fig. 6A). In addition, no significant difference was observed in extraosseous tumor volume upon BMP7 treatment (100 $\mu\text{g}/\text{kg}/\text{day}$) ($p = 0.15$; Fig. 5A). Furthermore, radiographic analysis of the tibiae revealed that mice receiving 100 $\mu\text{g}/\text{kg}/\text{day}$ BMP7 show significantly smaller bone lesions ($p = 0.046$), although number of osteoclasts per mm bone cortex appeared not to be different at the end of the experiment ($p = 0.528$; Fig. 5B). Systemic administration of BMP7 for the duration of the experiment can directly act on MDA-231-B/Luc+ bone metastatic cells as visualized by significantly enhanced nuclear staining for phospho-Smad1 when compared to vehicle treated animals ($p = 0.0097$; Fig. 5C).

Next, we studied the effects of BMP7 treatment on the growth of MDA-231-B/Luc+ cells that were orthotopically implanted into the mammary fat pads of nude mice (Fig. 6A-C). Fig. 6B depicts a representative example from both experimental groups (vehicle and 100 $\mu\text{g}/\text{kg}/\text{day}$ BMP7) as detected by BLI and histomorphometry. Tumor growth of the orthotopically implanted breast cancer cells in mice receiving 100 $\mu\text{g}/\text{kg}/\text{day}$ BMP7 was significantly inhibited versus vehicle treated animals ($p = 0.049$; Fig. 6C).

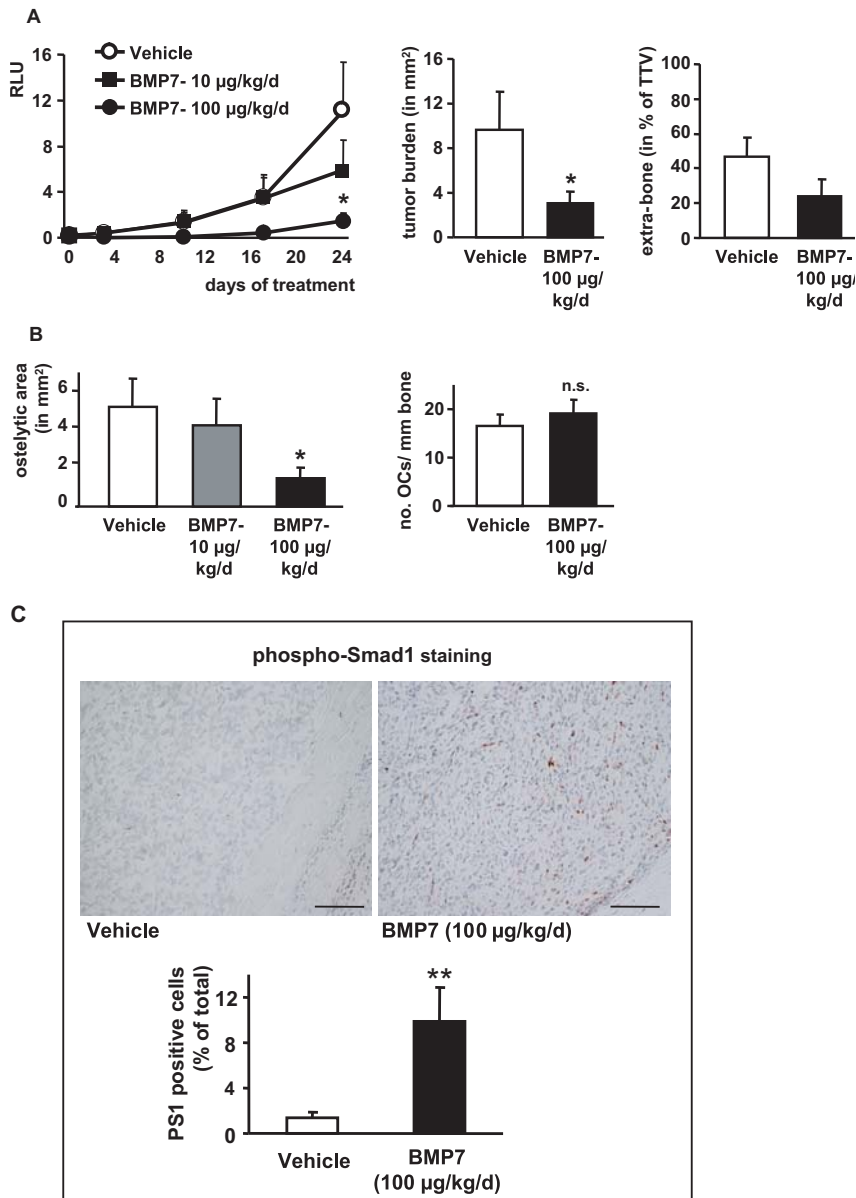


Figure 5 Effects of BMP7 treatment on intra-bone tumor growth, osteolysis and BMP7 signalling of MDA-231-B/Luc+ cells. **A**, tumor burden as measured by BLI (RLU: 10⁵ photons/sec) and histomorphometric analysis, and the extraosseous tumor volume determined as the percentage of total tumor volume (TTV) that has started to grow extramedullary. **B**, radiographical analysis of tumor-induced osteolysis in tibia at the end of the experimental treatment (24 days)(left), and number of osteoclasts (OCs) per mm bone cortex (right). **C**, phospho-Smad1 positive cells in the tumor at the end of the experimental treatment. The animals were either vehicle or BMP7 treated 6 hours prior explantation and fixation of the tibiae. Scale bars: 80 µm, * p < 0.05 and ** p < 0.01 versus vehicle.

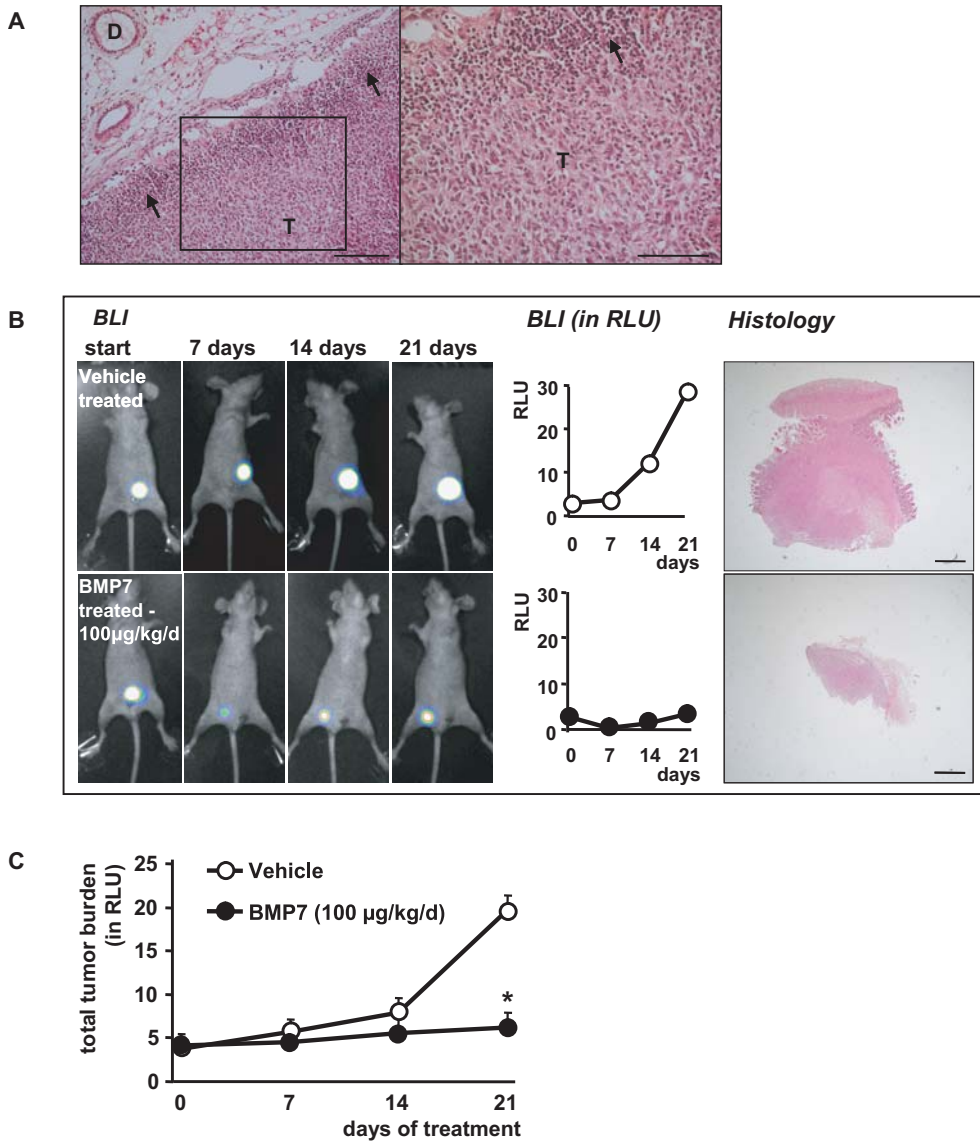


Figure 6 **BMP7 treatment and growth of MDA-231-B/Luc+ cells in mammary fat pads.** *A*, orthotopically implanted MDA-231-B/Luc+ cells have formed a tumor located in the mammary fat pad as shown by Hematoxylin & Eosin staining. The figure on the right is a magnification from the box in the left figure. Lymphocytic infiltrates (indicated by arrows) in tumors could be observed. Scale bar: 80 μm (left figure) and 50 μm (right figure); D = mammary duct, T = tumor. *B*, representative examples for BLI and HE staining are shown. BLI is quantified in RLU (10^5 photons/sec), scale bars: 500 μm. *C*) Tumor burden is measured by BLI (RLU: 10^5 photons/sec). * $p < 0.05$ versus vehicle.

Discussion

While BMP7 has been proposed as a marker of differentiation in normal and breast cancer cells⁴³, the role of BMP7 in breast cancer progression has remained largely elusive⁴³⁻⁴⁵. In this report novel evidence is provided for a role of BMP7 in breast cancer development and bone metastases. We describe here that BMP7 expression in patients with primary breast tumors exclusively developing bone metastases is significantly lower than in primary breast tumors developing exclusively visceral (lung and/or liver) metastases. These clinical findings suggest that decreased BMP7 expression may confer a bone metastatic potential to human breast cancer cells. Normal ducts of the breast display strong apical BMP7 protein expression. BMP7 protein expression in patient-matched lymph node metastases was low or absent, and as a consequence, generally lower than in normal ducts and primary breast carcinomas (J.T.Buijs, unpublished observations). Strikingly, BMP7 appears to be expressed predominantly in tumor cells in the solid tumor area rather than in migratory tumor cells outside this area⁴³, indicating that low BMP7 expression may support the acquisition of a more migratory invasive phenotype.

It has been well-established that the process of epithelial-to-mesenchymal transition (EMT) provides mechanisms for breast epithelial cells to overcome physical constraints imposed on them by intercellular junctions and adopt a motile phenotype^{3,8,46}. It is becoming increasingly clear that this local invasive process, representing initial stages of the metastatic cascade during carcinogenesis, is adapted from the remarkable epithelial plasticity (EMT) that occurs during embryonic development and postnatal tissue maintenance^{2,47}. In many cancers, TGF- β is a pro-tumorigenic factor that stimulates 'oncogenic' EMT^{8,17,18}. In contrast, BMP7 is a strong inducer of the reverse process (MET) during embryonic development^{9-11,14} and in renal fibroblasts²². Moreover, BMP7 can inhibit TGF- β -induced fibrosis²⁵, and counteracts TGF- β -induced EMT in normal renal epithelial cells²⁴.

We show here that BMP7 mRNA expression is inversely related to tumorigenicity and invasive behavior of human breast cancer cell lines. Functional studies reveal that BMP7 overexpression by breast cancer cells inhibits *de novo* formation of osteolytic bone metastases, and hence, the metastatic capability of breast cancer cells in our *in vivo* bone metastasis model. Furthermore, BMP7 overexpression significantly inhibited tumor growth in bone. In keeping with these functional data, daily systemic administration of BMP7 strongly and significantly impairs both the orthotopic and intraosseous growth of human MDA-231-B/Luc+breast cancer cells in nude mice.

Our *in vitro* studies reveal for the first time that BMP7 is a potent inhibitor of TGF- β -induced EMT in MDA-MB-231 cancer cells. In these cells, BMP7 is able of counteracting Smad-dependent TGF- β signaling. These actions of BMP7 may be of critical importance and could explain the observed beneficial effects of experimental BMP7 treatment on orthotopic growth and skeletal metastasis. In this context it is important to note that inactive TGF- β is

concentrated and stored in high amounts in extracellular bone matrix, and can be released and activated by osteoclastic resorption. Activated bone matrix-derived TGF- β may act as a paracrine growth factor for neighboring osteolytic cancer cells that may have colonized the bone marrow^{21,40,48}. Our *in vivo* data further support this notion since BMP7 antagonizes TGF- β signaling routes in human breast cancer cells that are metastatic to the skeleton. We hypothesize that the activation process of micrometastases in bone marrow may bear similarities to EMT that occurs at the primary site in various epithelial cancers and during ontogeny⁴⁹.

BMP7, however, could not restore E-cadherin expression in MDA-231-B/Luc+ cells. Recent observations support the notion that hypermethylation of the E-cadherin promoter in MDA-MB-231 cells is involved in E-cadherin expression⁶. Apparently, BMP7 can not overcome this epigenetic effect.

It is important to note that comparable data have been obtained in clinical samples of prostate cancer⁵⁰ and uveal melanoma⁵¹. Moreover, in human prostate cancer we recently observed that BMP7 antagonizes TGF- β induced EMT concomitant with an induction of E-cadherin expression⁵⁰.

Collectively, our data suggest that BMP7 regulates epithelial homeostasis in the human mammary gland by preserving the epithelial phenotype. Decreased BMP7 expression during breast cancer progression may, therefore, contribute to the acquisition of a bone metastatic phenotype. Furthermore, exogenous BMP7 can still inhibit breast cancer growth at the primary site and in bone marrow. Therefore, BMP7 may represent a novel therapeutic molecule for repression of local and bone metastatic growth of human breast cancer.

Acknowledgments

This work was supported by grants from Dutch Cancer Society (KWF project RUL-2001-2485) and European Sixth Framework Programme, MetaBre, FP6-503049).

References

1. Sporn MB. The war on cancer. *Lancet* 1996; 347:1377-81.
2. Thiery JP. Epithelial-mesenchymal transitions in development and pathologies. *Curr Opin Cell Biol* 2003; 15:740-6.
3. Hay ED. An overview of epithelio-mesenchymal transformation. *Acta Anat (Basel)* 1995; 154:8-20.
4. Grunert S, Jechlinger M, Beug H. Diverse cellular and molecular mechanisms contribute to epithelial plasticity and metastasis. *Nat Rev Mol Cell Biol* 2003; 4:657-65.
5. Dandachi N, Hauser-Kronberger C, More E, Wiesener B, Hacker GW, Dietze O *et al.* Co-expression of tenascin-C and vimentin in human breast cancer cells indicates phenotypic transdifferentiation during tumour progression: correlation with histopathological parameters, hormone receptors, and oncoproteins. *J Pathol* 2001; 193:181-9.

6. Lombaerts M, van Wezel T, Philippo K, Dierssen JW, Zimmerman RM, Oosting J *et al.* E-cadherin transcriptional downregulation by promoter methylation but not mutation is related to epithelial-to-mesenchymal transition in breast cancer cell lines. *Br J Cancer* 2006; 94:661-71.
7. Siitonen SM, Kononen JT, Helin HJ, Rantala IS, Holli KA, Isola JJ. Reduced E-cadherin expression is associated with invasiveness and unfavorable prognosis in breast cancer. *Am J Clin Pathol* 1996; 105:394-402.
8. Thiery JP. Epithelial-mesenchymal transitions in tumour progression. *Nat Rev Cancer* 2002; 2:442-54.
9. Dudley AT, Lyons KM, Robertson EJ. A requirement for bone morphogenetic protein-7 during development of the mammalian kidney and eye. *Genes Dev* 1995; 9:2795-807.
10. Luo G, Hofmann C, Bronckers AL, Sohocki M, Bradley A, Karsenty G. BMP-7 is an inducer of nephrogenesis, and is also required for eye development and skeletal patterning. *Genes Dev* 1995; 9:2808-20.
11. Vukicevic S, Kopp JB, Luyten FP, Sampath TK. Induction of nephrogenic mesenchyme by osteogenic protein 1 (bone morphogenetic protein 7). *Proc Natl Acad Sci U S A* 1996; 93:9021-6.
12. Ducy P, Karsenty G. The family of bone morphogenetic proteins. *Kidney Int* 2000; 57:2207-14.
13. Itoh S, Itoh F, Goumans MJ, Ten Dijke P. Signaling of transforming growth factor-beta family members through Smad proteins. *Eur J Biochem* 2000; 267:6954-67.
14. Simic P, Vukicevic S. Bone morphogenetic proteins in development and homeostasis of kidney. *Cytokine Growth Factor Rev* 2005; 16:299-308.
15. Oft M, Peli J, Rudaz C, Schwarz H, Beug H, Reichmann E. TGF-beta1 and Ha-Ras collaborate in modulating the phenotypic plasticity and invasiveness of epithelial tumor cells. *Genes Dev* 1996; 10:2462-77.
16. Roberts AB, Wakefield LM. The two faces of transforming growth factor beta in carcinogenesis. *Proc Natl Acad Sci U S A* 2003; 100:8621-3.
17. Peinado H, Quintanilla M, Cano A. Transforming growth factor beta-1 induces snail transcription factor in epithelial cell lines: mechanisms for epithelial mesenchymal transitions. *J Biol Chem* 2003; 278:21113-23.
18. Piek E, Moustakas A, Kurisaki A, Heldin CH, Ten Dijke P. TGF-(beta) type I receptor/ALK-5 and Smad proteins mediate epithelial to mesenchymal transdifferentiation in NMuMG breast epithelial cells. *J Cell Sci* 1999; 112:4557-68.
19. Yingling JM, Blanchard KL, Sawyer JS. Development of TGF-beta signalling inhibitors for cancer therapy. *Nat Rev Drug Discov* 2004; 3:1011-22.
20. Deckers M, van Dinther M, Buijs J, Que I, Lowik C, van der Pluijm G *et al.* The tumor suppressor Smad4 is required for transforming growth factor beta-induced epithelial to mesenchymal transition and bone metastasis of breast cancer cells. *Cancer Res* 2006; 66:2202-9.
21. Yin JJ, Selander K, Chirgwin JM, Dallas M, Grubbs BG, Wieser R *et al.* TGF-beta signaling blockade inhibits PTHrP secretion by breast cancer cells and bone metastases development. *J Clin Invest* 1999; 103:197-206.
22. Zeisberg M, Shah AA, Kalluri R. Bone morphogenetic protein-7 induces mesenchymal to epithelial transition in adult renal fibroblasts and facilitates regeneration of injured kidney. *J Biol Chem* 2005; 280:8094-100.
23. Hruska KA, Guo G, Wozniak M, Martin D, Miller S, Liapis H *et al.* Osteogenic protein-1 prevents renal fibrogenesis associated with ureteral obstruction. *Am J Physiol Renal Physiol* 2000; 279:F130-F143.
24. Zeisberg M, Hanai J, Sugimoto H, Mammoto T, Charytan D, Strutz F *et al.* BMP-7 counteracts TGF-beta1-induced epithelial-to-mesenchymal transition and reverses chronic renal injury. *Nat Med* 2003; 9:964-8.
25. Wang S, Hirschberg R. BMP7 antagonizes TGF-beta -dependent fibrogenesis in mesangial cells. *Am J Physiol Renal Physiol* 2003; 284:F1006-F1013.
26. Gould SE, Day M, Jones SS, Dorai H. BMP-7 regulates chemokine, cytokine, and hemodynamic gene expression in proximal tubule cells. *Kidney Int* 2002; 61:51-60.

27. Li T, Surendran K, Zawaideh MA, Mathew S, Hruska KA. Bone morphogenetic protein 7: a novel treatment for chronic renal and bone disease. *Curr Opin Nephrol Hypertens* 2004; 13:417-22.
28. Wetterwald A, van der Pluijm G, Que I, Sijmons B, Buijs J, Karperien M *et al.* Optical imaging of cancer metastasis to bone marrow: a mouse model of minimal residual disease. *Am J Pathol* 2002; 160:1143-53.
29. Soule HD, Maloney TM, Wolman SR, Peterson WD, Jr., Brenz R, McGrath CM *et al.* Isolation and characterization of a spontaneously immortalized human breast epithelial cell line, MCF-10. *Cancer Res* 1990; 50:6075-86.
30. Santner SJ, Dawson PJ, Tait L, Soule HD, Eliason J, Mohamed AN *et al.* Malignant MCF10CA1 cell lines derived from premalignant human breast epithelial MCF10AT cells. *Breast Cancer Res Treat* 2001; 65:101-10.
31. Peyruchaud O, Winding B, Pecheur I, Serre CM, Delmas P, Clezardin P. Early detection of bone metastases in a murine model using fluorescent human breast cancer cells: application to the use of the bisphosphonate zoledronic acid in the treatment of osteolytic lesions. *J Bone Miner Res* 2001; 16:2027-34.
32. Notting IC, Buijs JT, Que I, Mintardjo RE, van der HG, Karperien M *et al.* Whole-body bioluminescent imaging of human uveal melanoma in a new mouse model of local tumor growth and metastasis. *Invest Ophthalmol Vis Sci* 2005; 46:1581-7.
33. Bieche I, Parfait B, Le Doussal V, Olivi M, Rio MC, Lidereau R *et al.* Identification of CGA as a novel estrogen receptor-responsive gene in breast cancer: an outstanding candidate marker to predict the response to endocrine therapy. *Cancer Res* 2001; 61:1652-8.
34. Livak KJ, Schmittgen TD. Analysis of relative gene expression data using real-time quantitative PCR and the 2(-Delta Delta C(T)) Method. *Methods* 2001; 25:402-8.
35. Jones WK, Richmond EA, White K, Sasak H, Kusmik W, Smart J *et al.* Osteogenic protein-1 (OP-1) expression and processing in Chinese hamster ovary cells: isolation of a soluble complex containing the mature and pro-domains of OP-1. *Growth Factors* 1994; 11:215-25.
36. Deckers MM, Karperien M, van der Bent C, Yamashita T, Papapoulos SE, Lowik CW. Expression of vascular endothelial growth factors and their receptors during osteoblast differentiation. *Endocrinology* 2000; 141:1667-74.
37. Dennler S, Itoh S, Vivien D, Ten Dijke P, Huet S, Gauthier JM. Direct binding of Smad3 and Smad4 to critical TGF beta-inducible elements in the promoter of human plasminogen activator inhibitor-type 1 gene. *EMBO J* 1998; 17:3091-100.
38. Korchynskiy O, Ten Dijke P. Identification and functional characterization of distinct critically important bone morphogenetic protein-specific response elements in the Id1 promoter. *J Biol Chem* 2002; 277:4883-91.
39. van der Pluijm G, Que I, Sijmons B, Buijs JT, Lowik CW, Wetterwald A *et al.* Interference with the microenvironmental support impairs the de novo formation of bone metastases in vivo. *Cancer Res* 2005; 65:7682-90.
40. van der Pluijm G, Sijmons B, Vloedgraven H, Deckers M, Papapoulos S, Lowik C. Monitoring metastatic behavior of human tumor cells in mice with species-specific polymerase chain reaction: elevated expression of angiogenesis and bone resorption stimulators by breast cancer in bone metastases. *J Bone Miner Res* 2001; 16:1077-91.
41. Chubinskaya S, Merrihew C, Cs-Szabo G, Mollenhauer J, McCartney J, Rueger DC *et al.* Human articular chondrocytes express osteogenic protein-1. *J Histochem Cytochem* 2000; 48:239-50.
42. Persson U, Izumi H, Souchelnytskyi S, Itoh S, Grimsby S, Engstrom U *et al.* The L45 loop in type I receptors for TGF-beta family members is a critical determinant in specifying Smad isoform activation. *FEBS Lett* 1998; 434:83-7.
43. Schwalbe M, Sanger J, Eggers R, Naumann A, Schmidt A, Hoffken K *et al.* Differential expression and regulation of bone morphogenetic protein 7 in breast cancer. *Int J Oncol* 2003; 23:89-95.
44. Alarmo EL, Rauta J, Kauraniemi P, Karhu R, Kuukasjarvi T, Kallioniemi A. Bone morphogenetic protein 7 is widely overexpressed in primary breast cancer. *Genes Chromosomes Cancer* 2006; 45:411-9.

45. Bobinac D, Maric I, Zoricic S, Spanjol J, Dordevic G, Mustac E *et al.* Expression of bone morphogenetic proteins in human metastatic prostate and breast cancer. *Croat Med J* 2005; 46:389-96.
46. Vincent-Salomon A, Thiery JP. Host microenvironment in breast cancer development: epithelial-mesenchymal transition in breast cancer development. *Breast Cancer Res* 2003; 5:101-6.
47. Savagner P, Kusewitt DF, Carver EA, Magnino F, Choi C, Gridley T *et al.* Developmental transcription factor slug is required for effective re-epithelialization by adult keratinocytes. *J Cell Physiol* 2005; 202:858-66.
48. Mundy GR. Metastasis to bone: causes, consequences and therapeutic opportunities. *Nat Rev Cancer* 2002; 2:584-93.
49. Bryden AA, Freemont AJ, Clarke NW, George NJ. Paradoxical expression of E-cadherin in prostatic bone metastases. *BJU Int* 1999; 84:1032-4.
50. Buijs JT, Rentsch CA, van der Horst G, van Overveld PGM, Wetterwald A, Schwaninger R *et al.* BMP7, a Putative Regulator of Epithelial Homeostasis in the Human Prostate, is a Potent Inhibitor of Prostate Cancer Bone Metastasis In Vivo. *Am J Pathol* 2007; 171:1047-57.
51. Notting I, Buijs J, Mintardjo R, van der Horst G, Vukicevic S, Lowik C *et al.* Bone morphogenetic protein 7 inhibits tumor growth of human uveal melanoma in vivo. *Invest Ophthalmol Vis Sci* 2007; 48:4882-9.

